[Research Paper] 대한금속 · 재료학회지 (*Korean J. Met. Mater.*), Vol. 61, No. 6 (2023) pp.431-436
DOI: 10.3365/KJMM.2023.61.6.431

Enhanced Thermoelectric Transport Properties in Cu-added Bi_2Se_3 Polycrystalline Alloys

Hyungyu Cho[1,†], TaeWan Kim[2,†], Seung Min Kang[1], Sanghyun Park[1], and Sang-il Kim[1,*]

[1]*Department of Materials Science and Engineering, University of Seoul, Seoul 02504, South Korea*
[2]*Department of Electrical Engineering and Smart Grid Research Center, Jeonbuk National University, Jeonju 54896, South Korea*

Abstract: The addition of Cu to layered Bi_2Te_3-based thermoelectric alloys has been studied as an effective way to enhance thermoelectric transport properties. In this study, the influence of adding Cu to Bi_2Se_3 alloys, which have the same rhombohedral crystal structure as Bi_2Te_3, was investigated by synthesizing a series of $Cu_xBi_2Se_3$ (x = 0, 0.004, 0.008, 0.012, and 0.016) alloys. The power factors of all the Cu-added samples were enhanced compared with that of the pristine Bi_2Se_3 sample, primarily because of the increase in electrical conductivity. The power factor for the $Cu_{0.016}Bi_2Se_3$ sample (x = 0.016) was 0.80 mW/mK^2, a 35% increase compared to 0.59 mW/mK^2 for the pristine sample at 520 K. A decrease in the total and lattice thermal conductivity was observed for the Cu-added samples, caused by additional point defect scattering after doping. The lattice thermal conductivity of the $Cu_{0.016}Bi_2Se_3$ sample (x = 0.016) was 0.56 W/mK, a 42% reduction. Consequently, the zT values of all the Cu-added samples were enhanced, and the maximum zT value was 0.38 for the $Cu_{0.016}Bi_2Se_3$ sample (x = 0.016) at 520 K, a 48% increase compared to that of pristine Bi_2Se_3. The phenomenological transport parameters, including density of state, effective mass, weighted mobility, and thermoelectric quality factor, were calculated to analyze the enhanced electronic transport properties of the Cu-added Bi_2Se_3.

(Received 2 February, 2023; Accepted 28 February, 2023)

Keywords: thermoelectric, Bi_2Se_3, Cu doping

1. INTRODUCTION

Thermoelectric materials have attracted significant attention as eco-friendly and sustainable energy production technologies because of their ability of convert heat to electricity through the Seebeck effect [1-3]. The thermoelectric efficiency of materials is expressed as a dimensionless figure of merit, $zT = S^2\sigma T/\kappa_{tot}$, where σ, S, κ_{tot}, and T are the electrical conductivity, Seebeck coefficient, thermal conductivity, and absolute temperature, respectively. To enhance zT, σ and S must be increased while κ_{tot} must be decreased. However, it is not simple to enhance zT because of trade-off relationship between σ and S. Therefore, a lot of tactics such as band structure engineering, carrier scattering and nanostructing have been studied to increase zT [4-6].

The Bi-Te alloy is a representative chalcogenide with high thermoelectric performance in the room-temperature range. Because of their low thermal conductivity and relatively high electrical conductivity, Bi-Te alloys are used for cooling systems in small-scale thermoelectric generation modules in the low-temperature range [7]. The Bi_2Te_3 in Bi-Te alloys has a trigonal crystal structure with a quintuple-layer structure that is stacked repeatedly in the order of Te-Bi-Te-Bi-Te in the c-axis direction. Because it has strong covalent bonds and ionic bonds in the ab-plane direction and Van der Waals bonds in the c-axis direction, Bi_2Te_3 has outstanding electrical performance with high σ, high S, and low κ_{tot}.

Bismuth selenide (Bi_2Se_3), which is one of the chalcogenides and has the same rhombohedral structure as Bi_2Te_3, has been widely studied as a thermoelectric material as well [8-9]. Kang et al. reported that polycrystalline Bi_2Se_3 exhibited a zT value of 0.12 at room temperature [10]. Sun et al. reported that single-layer-based Bi_2Se_3 exhibited a zT value of 0.1 at room temperature and a maximum zT value of

[†]These authors contributed equally to this study.
- 조현규 · 강승민 · 박상현: 학사과정, 김태완 · 김상일: 교수
**Corresponding Author:* Sang-il Kim
[Tel: +82-2-6490-2414, E-mail: sang1.kim@uos.ac.kr]

0.35 at 400 K [11]. Hong et al. reported that Bi_2Se_3 nanosheets exhibited a zT value of 0.17 at room temperature and a maximum zT value of 0.48 at 427 K [12]. Because the experimentally reported thermoelectric performance of Bi_2Se_3 is low, several attempts have been made to increase that thermoelectric performance, with one of them by doping [13-14]. Li et al. doped Bi_2Se_3 with Sn using the composition $Bi_{1.93}Sn_{0.07}Se_3$ and obtained a zT increase of 60% compared with that of pure Bi_2Se_3 [15]. P. Janíček et al. reported that doping Bi_2Se_3 with thallium enhanced the power factor by 25% [16].

Meanwhile, adding Cu to Bi_2Te_3 has been reported to enhance the thermoelectric performance [17-18]. Kim et al. reported that Bi_2Te_3 with Cu addition enhanced thermoelectric performance and improved electronic transport properties [19]. In this study, the thermoelectric transport properties of Cu-added Bi_2Se_3 polycrystalline alloys were investigated because Bi_2Se_3 has the same structure as Bi_2Te_3 in the bismuth chalcogenide family. The thermoelectric transport properties, including σ, S, and κ_{tot}, were measured, and the phenomenological transport parameters, including density of state effective mass (m_d^*), weighted mobility (μ_w), and thermoelectric quality factor (B), were calculated to analyze the electronic transport properties of the Cu-added Bi_2Se_3.

2. EXPERIMENTAL

$Cu_xBi_2Se_3$ (x = 0, 0.004, 0.008, 0.012, and 0.016) polycrystalline samples were stoichiometrically synthesized via a solid-state reaction. High-purity elemental Bi (99.999%), Se (99.999%), and Cu (99.998%) powders were mixed and loaded into vacuum quartz tubes. After melting at 800 ºC for 4 h, the samples were cooled to room temperature in a furnace. The synthesized ingot samples were pulverized into powders by high-energy ball milling (SPEX 8000D, SPEX). The samples were sintered via spark plasma sintering (SPS, SPS-1030, Sumitomo Coal Mining Co., Ltd., Japan) under vacuum at 350 ºC for 10 min at 70 MPa. The crystalline phase of the samples was identified by X-ray diffraction (XRD, D8 Discover, Bruker) with Cu $K_{\alpha1}$ radiation at 40 kV and 40 mA. The values of S and σ were measured using a thermoelectric evaluation system (ZEM-3M8, Advance Riko, Japan) along the perpendicular direction of the SPS pressing direction in a He atmosphere. Hall measurement was performed at room temperature in the same direction using the Van der Pauw method to determine the carrier concentration (n_H) and mobility (μ_H). The κ_{tot} value of the samples was calculated using the theoretical density (ρ_s), heat capacity (C_p), and thermal diffusivity (λ) ($\kappa_{tot} = \rho_s C_p \lambda$). The λ value of each sample was measured by laser flash system analysis (LFA457, Netsch). The zT values of the samples were calculated based on measured data.

3. RESULTS AND DISCUSSION

Figure 1(a) and (b) show the XRD patterns of the sintered $Cu_xBi_2Se_3$ samples (x = 0, 0.004, 0.008, 0.012, and 0.016). As shown in Figure 1(a), a single-phase Bi_2Se_3 with a rhombohedral structure was synthesized without impurities. Figure 1(b) shows the lattice parameters a and c calculated from the XRD data with error bars. No variation was observed in the lattice parameter a with the varying Cu content. However, the lattice parameter c varied with the Cu content, increasing from 28.64 to 28.67 Å as x varied from 0 to 0.008, and then exhibiting a decreasing tendency beyond x = 0.008. This behavior was also observed in the study of Cu doping of Bi_2Te_3 [19]; Cu was intercalated into the van der Waals gap of Bi_2Te_3 (lattice parameter c increased) with small Cu additions, while Cu also entered the substitutional site of Bi (lattice parameter c decreased). Thus, it was speculated that the increase in the lattice parameter c up to x = 0.008 can be attributed to Cu intercalation, and the decrease beyond x = 0.008 is due to Cu substitution of Bi site.

Figure 2(a) shows the temperature dependence of σ.

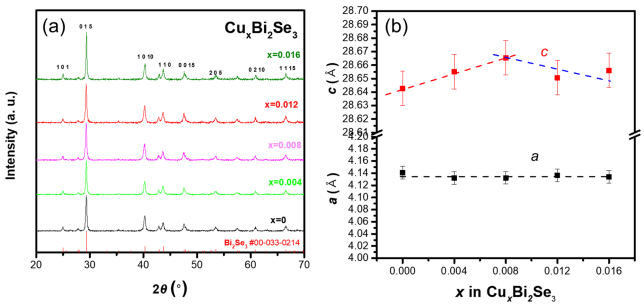

Fig. 1. (a) XRD patterns of the $Cu_xBi_2Se_3$ (x = 0, 0.004, 0.008, 0.012, 0.016) samples and (b) lattice parameters calculated from the XRD data.

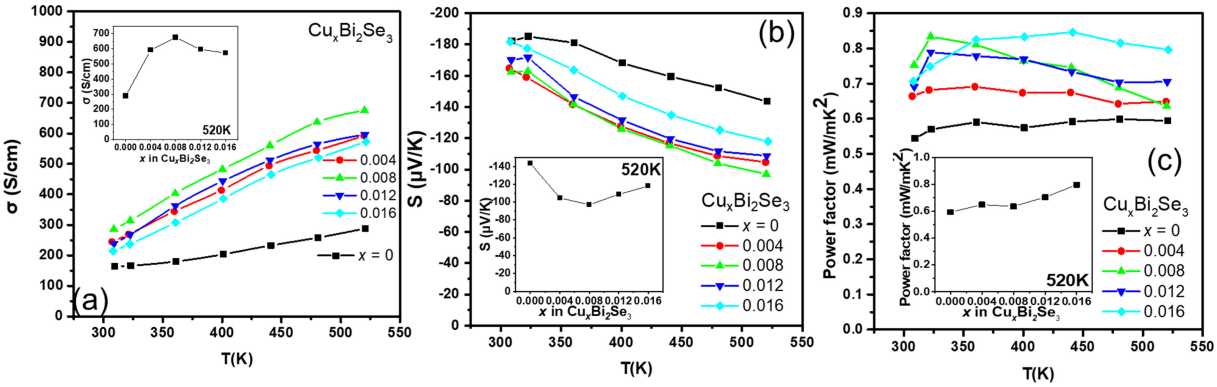

Fig. 2. (a) Electrical conductivity as a function of temperature for the Cu_xBi2Se3 (x = 0, 0.004, 0.008, 0.012, 0.016) samples. The inset of (a) shows the σ values at 520 K as a function of Cu doping content (x). (b) Seebeck coefficient as a function of temperature. The inset of (b) shows the S values at 520 K as a function of the Cu doping content (x). (c) Power factor as a function of temperature. The inset of (c) shows the power factor values at 520 K as a function of Cu doping content (x).

Semiconducting conduction behavior was observed for all samples, as σ increased with temperature. Moreover, the value of σ for the $Cu_xBi_2Se_3$ samples (x = 0.004, 0.008, 0.012, 0.016) was higher than that of the pristine Bi_2Se_3. At 300 K, the value of σ for the pristine Bi_2Se_3 sample was 164 S/cm, and it increased to 245, 286, 239, and 214 S/cm for the samples with x = 0.004, 0.008, 0.012, and 0.016, respectively. The inset of Figure 2(a) shows the σ values as a function of x at 520 K, indicating that the σ values of all the Cu-added samples were higher than that of the pristine Bi_2Se_3 sample.

Furthermore, the results in the inset of Figure 2(a) are similar to those of a previous study that showed that the increase in the value of σ up to x = 0.008 was due to Cu occupying the interstitial sites, and the decrease beyond x = 0.008 was attributed to the substitution of Cu in the Bi site [19]. Figure 2(b) shows the temperature dependence of the S of the samples, the negative values of S indicate that all the samples are n-type semiconductors. The S values of all the Cu-added samples were smaller than that of the pristine Bi_2Se_3 sample over the entire temperature range. The inset of Figure 2(b) shows the S values as a function of x at 520 K, indicating that the S values of the Cu-added samples were lower than that of pristine Bi_2Se_3. Similar results were obtained in a previous study that showed that the decrease in S values up to x = 0.008 indicates interstitial site doping, and the increase beyond x = 0.008 indicates interstitial and substitutional doping [19].

Figure 2(c) shows the power factor values of the samples calculated from the measured σ and S values. The power factor values of the Cu-added samples were higher than that of the pristine Bi_2Se_3 sample at all measured temperatures. The maximum power factor values were observed for $Cu_{0.008}Bi_2Se_3$ sample 0.83 mW/mK^2 in the lower temperature range (T < 360 K). However, in the high temperature range, the maximum power factor values were observed for $Cu_{0.016}Bi_2Se_3$ sample (T > 360 K). The power factor values of the pristine Bi_2Se_3 sample improved, from 0.54 to 0.83 mW/mK^2 (x = 0.008), at room temperature and from 0.59 to 0.80 mW/mK^2 (x = 0.016) at 520 K (inset of Figure 2(c).

Figure 3(a) and (b) show the measured Hall carrier concentration (n_H) and Hall mobility (μ_H) of the samples at 300 K. As shown in Figure 3(a), n_H increased from 1.94 × 10^{18} to 2.81 × 10^{18} cm^{-3} owing to a small amount of Cu doping ($Cu_{0.008}Bi_2Te_3$), then decreased to 2.17 × 10^{18} cm^{-3} beyond x = 0.008. Based on a previous study, it can be speculated that excess Cu atoms are preferentially located at the van der Waals gap in the sample with lower Cu content ($x \le 0.008$), while incorporated Cu atoms at Bi-site occur in the samples with higher Cu content beyond x = 0.008 [19]. Figure 1(b) shows good agreement with these results because the ionic radii of Cu^{1+} and $Cu^{2+}$are smaller than that of Bi^{3+}. Figure 3(b) shows the μ_H values measured at 300 K. The μ_H of the samples were 605, 755, 658, 741, and 685 cm^2/Vs for x = 0, 0.004, 0.008, 0.012, and 0.016, respectively.

Figure 3(c) shows the weighted mobility (μ_w) as a function of temperature for the samples. μ_w is proportional to the maximum power factor that a sample can attain when n_H is

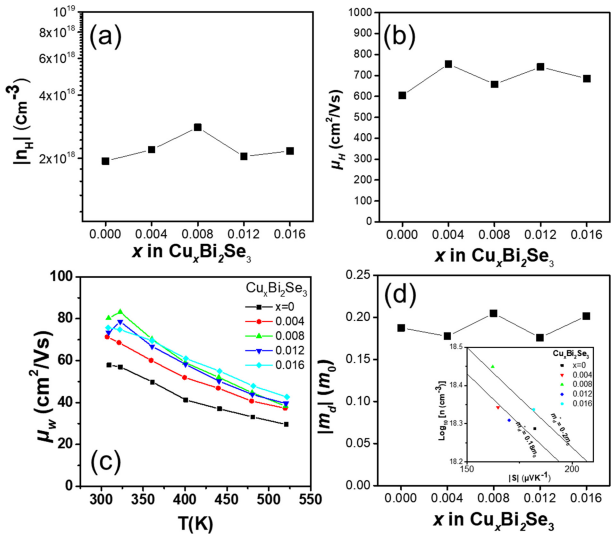

Fig. 3. (a) Hall carrier concentration and Hall mobility of the $Cu_xBi_2Se_3$ (x = 0, 0.004, 0.008, 0.012, 0.016) samples at 300 K. (c) Weighted mobility as a function of temperature for the samples and (d) the calculated effective mass m_d^* as a function of the Cu doping content (x). The inset of (d) shows the Seebeck coefficient as a function of the measured carrier concentration (Pisarenko plot) at 300 K.

optimized. The μ_w value of each sample was calculated from the measured σ and S using a simple analytical form that approximates the exact Drude-Sommerfield free-electron model given in Equation (1) for $|S|>20$ μV/K [20].

$$\mu_w = \frac{3h^3\sigma}{8\pi e(2m_e kT)^{3/2}}$$

$$\left[\frac{exp\left[\frac{|S|}{k/e}-2\right]}{1+\exp\left[-5\left(\frac{|S|}{k/e}-1\right)\right]}+\frac{\frac{3|S|}{\pi^2 k/e}}{1+exp\left[5\left(\frac{|S|}{k/e}-1\right)\right]}\right] \quad (1)$$

where m_e is the electronic mass. The calculated μ_w values at 520 K were 29.5, 37.3, 38.3, 39.5; and 42.7 cm^2/Vs for x = 0, 0.004, 0.008, 0.012; and 0.016, respectively. The μ_w value increases as the Cu content increases, which is in agreement with the power factor trend over the whole temperature range.

Figure 3(d) shows the calculated m_d^* of the $Cu_xBi_2Se_3$ (x = 0, 0.004, 0.008, 0.012, and 0.016) samples with respect to x. The inset of Figure 3(d) shows $\log_{10}n_H$ as a function of $|S|$. The m_d^* values were calculated based on a single parabolic band model using an acoustic phonon-scattering mechanism [20].

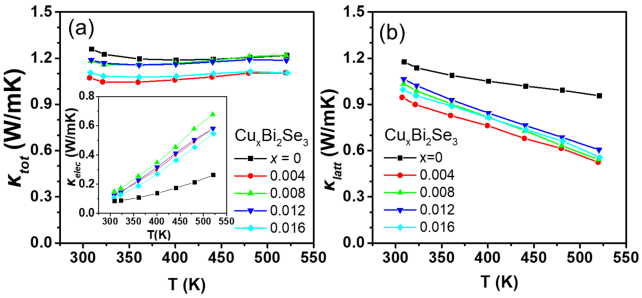

Fig. 4. (a) Total thermal conductivity as a function of temperature for the $Cu_xBi_2Se_3$ (x = 0, 0.004, 0.008, 0.012, 0.016) samples. The inset of (a) shows the electronic thermal conductivity. (b) Lattice thermal conductivity as a function of temperature

$$\log_{10}\left(\frac{m_d^* T}{300}\right) = \frac{2}{3}\log_{10}(n_H) - \frac{2}{3}[20.3-(0.00508\times|S|)+(1.58\times 0.967^{|S|})] \quad (2)$$

The m_d^* values of the samples were 0.187, 0.177, 0.205, 0.176 and 0.202 m_0 for x = 0, 0.004, 0.008, 0.012 and 0.016, respectively. It can be speculated that the m_d^* value increased because of Cu intercalation for x = 0 to at x = 0.008, and that it decreased because of Cu substitution for x = 0.012 and 0.016, based on a previous study [19].

Figure 4(a) and (b) show the κ_{tot} and lattice thermal conductivity (κ_{latt}) as a function of temperature for the $Cu_xBi_2Se_3$ (x = 0, 0.004, 0.008, 0.012, 0.016) samples. The inset of Figure 4(a) shows the electronic thermal conductivity (κ_{elec}), calculated using the Wiedemann Franz law [21]: $\kappa_{elec} = L\sigma T$, where L is the Lorenz number. L is calculated using the equation L = 1.5 + exp(-|S|/116) (where L is in 10^{-8} $W\Omega K^{-2}$ and S in μV/K) [22]. The κ_{latt} value was obtained by subtracting κ_{elec} from κ_{tot}. The κ_{latt} values for the Cu-added samples were lower than that of the pristine Bi_2Se_3 sample over the entire temperature range. The κ_{latt} value significantly decreased from 0.96 W/mK for the pristine sample to 0.52–0.61 W/mK for Cu-added samples at 520 K. The decrease in the κ_{latt} values with Cu content is due to point defect phonon scattering caused by the Cu addition.

Figure 5(a) shows the temperature dependence of zT for each sample calculated from the σ, S, and κ_{tot} values. As shown in Figure 5(a), the zT value of the Cu-added Bi_2Se_3 samples were higher than that of the pristine Bi_2Se_3 sample. The highest zT value (0.38) was achieved for the sample with

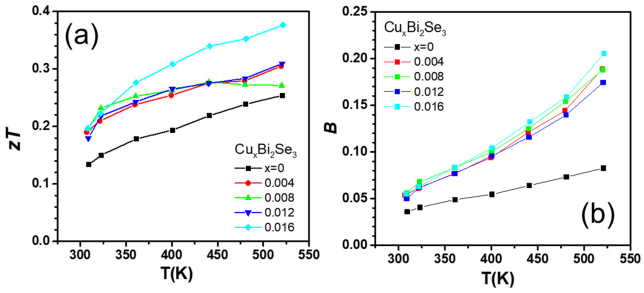

Fig. 5. (a) Thermoelectric figure of merit zT as a function of temperature for the $Cu_xBi_2Se_3$ (x = 0, 0.004, 0.008, 0.012, 0.016) samples. (b) Quality factor as a function of temperature

x = 0.016 at 520 K, which was ~48% higher than that of the pristine Bi_2Se_3 sample. The increase in zT for all samples over whole temperature range was attributed to the increase in the power factor and decrease in κ_{latt}.

Figure 5(c) shows the dimensionless thermoelectric quality factor (B) of each sample, calculated from μ_w and κ_{latt}. B is related to the maximum zT that a material can achieve when n_H is optimized; B was calculated using Equation (3) [20] as follows:

$$B = \left(\frac{k}{e}\right)^2 \left(\frac{8\pi e(2m_e kT)^{3/2}}{3h^3} \cdot \frac{\mu_w}{\kappa_{latt}} T \right) \quad (3)$$

The value of B at 520 K were 0.083, 0.19, 0.19, 0.17 and 0.21 for x = 0, 0.004, 0.008, 0.012 and 0.016, respectively. Therefore, a zT improvement can be expected for all Cu-added samples, and was probably maximized at 520 K for x = 0.012 when n_H is optimized.

4. CONCLUSIONS

The thermoelectric transport properties of Cu-added Bi_2Se_3 ($Cu_xBi_2Se_3$, x = 0, 0.004, 0.008, 0.012, and 0.016) were investigated. A rhombohedral Bi_2Se_3 phase was synthesized without secondary phases. Cu doping increases the electrical conductivity and carrier concentration. As a result, the power factor values of the samples increases from 0.54 (x = 0) to 0.83 mW/mK^2 (x = 0.008) at room temperature and 0.59 (x = 0) to 0.80 mW/mK^2 (x = 0.016) at 520 K. A decrease in thermal conductivity was observed in the Cu-added samples because of the decrease in the lattice thermal conductivity. Consequently, the zT values of all Cu-added samples ($Cu_xBi_2Se_3$, x = 0.004, 0.008, 0.012, and 0.016) were enhanced compared with that of the pristine Bi_2Se_3 sample over the entire temperature range. The maximum zT value of 0.38 was observed for the $Cu_{0.016}Bi_2Se_3$ (x = 0.16) sample at 520 K, which exhibited a 48% improvement in zT compared with that of pristine Bi_2Se_3.

ACKNOWLEDGEMENT

This work was supported by the National Research Foundation of Korea (NRF-2021R1C1C1006147)

REFERENCES

1. M. P. Cenci, T. Scarazzato, D. D. Munchen, P. C. Dartora, H. M. Veit, A. M. Bernardes, and P. R. Dias, *Adv. Mater. Technol.* **7**, 2001263 (2022).
2. L. E. Bell, *Science* **321**, 1457 (2008).
3. X. F. Zheng, C. X. Liu, Y. Y. Yan, and Q. Wang, *Renew. Sust. Energ. Rev.* **32**, 486 (2014).
4. S. Kim and H. Kim, *Korean J. Met. Mater.* **59**, 127 (2021).
5. S. Kim, J. Lim, H. Yang, and H. Kim, *Korean J. Met. Mater.* **59**, 54 (2021)
6. A. J. Minnich, M. S. Dresselhaus, Z. F. Ren, and G. Chen, *Energy Environ. Sci.* **2**, 466 (2009).
7. S. I. Kim, K. H. Lee, H. A. Mun, H. S. Kim, S. W. Hwang, J. W. Roh, D. J. Yang, W. H. Shin, X. S. Li, Y. H. Lee, G. J. Snyder, and S. W. Kim, *Science* **348**, 109 (2015).
8. L. Wz, *Nanoscale Res. Lett.* (2011).
9. M. Hong, Z. Chen, L. Yang, G. Han, and J. Zou, *Adv. Electron. Mater.* **1** (2015).
10. Y. Kang, Q. Zhang, C. Fan, W. Hu, C. Chen, L. Zhang, F. Yu, Y. Tian, and B. Xu, *J. Alloys Compd.* **700**, 223 (2017).
11. Y. Sun, H. Cheng, S. Gao, Q. Liu, Z. Sun, C. Xiao, C. Wu, S. Wei, and Y. Xie, *J. Am. Chem. Soc.* **134**, 20294 (2012).
12. M. Hong, Z. Chen, L. Yang, G. Han, and J. Zou, *Adv. Electron. Mater.* **1** (2015).
13. G. Zhang and B. Li, *Nanoscale* **2**, 158 (2010).
14. M. M. Alsalama, H. Hamoudi, A. Abdala, Z. K. Ghouri, and K. M. Youssef, *Rev. Adv. Mater. Sci.* **59**, 371 (2020).
15. M. Li, Y. Zhang, T. Zhang, Y. Zuo, K. Xiao, J. Arbiol, J. Llorca, Y. Liu, and A. Cabot, *Nanomaterials* **11**, 1827 (2021).
16. P. Janicek, C. Drasar, L. Benes, and P. Los, *Cryst. Res. Technol. (1979)* **44**, 505 (2009).
17. M. Han, K. Ahn, H. Kim, J. Rhyee, and S. Kim, *J. Mater.*

Chem. A **21**, 11365 (2011).
18. H. Wu and W. Yen, *Acta Mater.* **157**, 33 (2018).
19. Y. H. Kim, Y. Kim, H. Kim, S. Choi, S. Kim, and K. H. Lee, *Int. J. Energy Res.* **46**, 3707 (2022).
20. G. J. Snyder, A. H. Snyder, M. Wood, R. Gurunathan, B. H. Snyder, and C. Niu, *Adv. Mater.* **32**, e2001537 (2020).
21. K. H. Lee, S. Kim, J. Lim, J. Y. Cho, H. Yang, and H. Kim, *Adv. Funct. Mater.* **32**, 2203852 (2022).
22. H. Kim, Z. M. Gibbs, Y. Tang, H. Wang, and G. J. Snyder, *APL Mater.* **3**, 41506 (2015).